ISSN 1063-7761, Journal of Experimental and Theoretical Physics, 2023, Vol. 137, No. 4, pp. 474–485. © Pleiades Publishing, Ltd., 2023.
Russian Text © The Author(s), 2023, published in Zhurnal Eksperimental'noi i Teoreticheskoi Fiziki, 2023, Vol. 164, No. 4, pp. 550–562.

Antiferromagnetic Excitonic Insulator

V. V. Val'kov[a,*]

[a] *Kirensky Institute of Physics, Siberian Branch, Russian Academy of Sciences, Krasnoyarsk, 660036 Russia*

**e-mail: vvv@iph.krasn.ru*

Received April 5, 2023; revised April 25, 2023; accepted April 29, 2023

Abstract—The effective the two-band Hamiltonian is obtained for iridium oxides with account for strong electron correlations (SEC) and the spin–orbit interaction. The intraatomic electron correlations in iridium ions induce the formation of Hubbard fermions (HF) filling the states in the valence band. Another consequence of SEC is associated with the emergence of the antiferromagnetic (AFM) exchange interaction between HF in accordance with the Anderson mechanism. As a result, a long-range antiferromagnetic order is established in the system, and in the conditions of band overlapping, the intersite Coulomb interaction induces a phase transition to the excitonic insulator (EI) state with a long-range AFM order. The system of integral self-consistent equations, the solution to which determines the excitonic order parameter components $\Delta_{i,j}(k)$, sublattice magnetization M, Hubbard fermion concentration n_d, and chemical potential μ, is obtained using the atomic representation, the method of two-time temperature Green's functions, and the Zwanzig–Mori projection technique. The symmetry classification of AFM EI phases is performed, and it is shown that in the nearest neighbor approximation, state $\Delta_{i,j}(k)$ with the s-type symmetry corresponds to the ground state, while the phases with the d- and p-symmetries are metastable.

DOI: 10.1134/S1063776123100138

1. INTRODUCTION

The study of materials in which a phase transition (PT) to the state with the long-range antiferromagnetic order occurs upon cooling [1] led to the formulation of a number of fundamental problems associated with manifestation of quantum effects on the macroscopic level. This concerns above all the problem of the ground state of the spin subsystem with the AFM ordering, analysis of the effect of quantum fluctuations on the stabilization of the equilibrium value of the sublattice magnetization [2], as well as the investigation of the behavior of AFM materials in a magnetic bonds [3–5].

The quantum nature of magnetic ordering manifests itself much more strongly in low-dimensional materials [6] as well as in compounds with a triangular lattice of magnetically active ions. In this case, the effect of quantum fluctuations [7, 8] determining qualitatively new features of antiferromagnets increases significantly because of frustrated bonds.

Apart from analysis of traditional insulators with the AFM ordering, the possibility of realization of the same magnetic order in materials in which the insulator state is induced from the semimetal state in accordance with the excitonic mechanism of electron–hole paring has been studied since the middle of 1960s.

It should be noted that the spin–singlet mechanism of the electron–hole coupling, which was proposed in [9–11], induced the excitonic insulator (EI) phase without a magnetic order. The realization of this mechanism requires the fulfillment of conditions associated with topological features of constant-energy surfaces of electrons and holes. This limited the class of materials in which the EI phase could exist and could be reliably identified. Nevertheless, the experimental data on optical and thermal properties of compounds such as Ta_2NiSe_5, which have been obtained and investigated in recent years [12], indicate the realization of the spin–singlet EI phase.

One of possible scenarios for the emergence of EIs with a long-range magnetic order is based on the spin-triplet electron–hole pairing accompanied with the emergence of a spin density wave (SDW). Detailed analysis of this interesting issue can be found in review [13].

The report [14] on the detection of features of the formation of the AFM order in $Sr_3Ir_2O_7$ in accordance with the excitonic mechanism stimulated investigations of the conditions for the realization of the antiferromagnetic excitonic insulator (AFM EI) phase.

Compound $Sr_3Ir_2O_7$ belongs to the class of iridium oxides characterized by general formula $Sr_{n+1}Ir_nO_{3n+1}$ with $n = 1, 2, \ldots$. These compounds are of considerable interest since their physical properties are formed under the simultaneous effect of the crystal field, the substantial spin–orbit interaction (SOI), and strong Hubbard correlations.

In view of the large spatial length of 5*d* electron states forming the iridium ion term, its octahedron surroundings (oxygen ions) leads to such a strong decrease in the energy of the split t_{2g} state, that it can become commensurate with the highest energy of filled oxygen orbitals. This ensures the overlapping of energy bands and creates favorable conditions of EI realization.

It is well known that SOI can play a significant role in the formation of nontrivial properties of the electronic energy structure. For example, we can mention topological insulators [15, 16], quantum spin liquids [17], as well as excitonic insulators with the $s + d$ type of the order parameter symmetry [18]. The latter case is distinguished by the fact that in spite of the trivial topology of the energy structure of Fermi states, edge states are realized in such dielectrics.

In compounds $Sr_{n+1}Ir_nO_{3n+1}$, the strong SOI and modifies the single-ion electron basis of iridium ion states leads to the formation of the lower fully occupied quartet and the split-off half-filled doublet with $J_{\text{eff}} = 1/2$ [19]. As a result, the quartet states stop affecting the characteristics of the system, and only the doublet states remain effective. This considerably simplifies the model of the electron structure of materials in question because of reduction of dimension of the Hilbert space basis.

It is important that such a reduction is accompanied with a decrease in the effective band width [20], leading to a relative increase in the intraatomic Hubbard repulsion. These factors ensure the regime in which SOI and SEC effects are manifested simultaneously [21, 22].

The above factors allows one to formulate the minimal two-band model of the electron energy structure of iridium oxide. In this model, SECs induce the exchange interaction of the antiferromagnetic type and ensure the possibility of realization of the antiferromagnetic excitonic insulator phase. Such a model allows one to consider basic characteristics of the ground state of the electron subsystem of $Sr_3Ir_2O_7$ in the AFM EI phase and to calculate the energy spectrum.

The article is organized as follows. In Section 2, the possibility of description of basic features of the AFM EI phase formation in iridium oxides is substantiated using the minimal two-band model. In Section 3, a transition is made to the atomic representation and the effective Hamiltonian, which allows one to take into account strong electron correlations and to describe the exchange AFM interaction in the Hubbard fermion subsystems. Section 4 is devoted to the derivation of the expression for the sublattice magnetization with account for the contributions associated with the motion of the Hubbard fermions over the lattice. In Section 5, the equations for the fermionic Green's functions (GF) are considered and the excitonic order parameter (EOP) components are introduced. The derivation of the self-consistent equations for these components is described in Section 6. In Section 7, the results of symmetry classification of solutions to the system of self-consistent integral equations are considered, which allows one to pass from the integral equations to the transcendental equations for EOP amplitudes. In Section 8, the solution with the *s*-type order parameter symmetry is considered and the features of the fermionic excitation spectrum in the AFM EI phase are analyzed. The quasi-momentum dependences of the weight contributions to the spectral intensity of the fermionic GF are also considered. These dependences explain the features of the formation of EOP components leading to the emergence of a dielectric gap with a transition of the system to the AFM EI state. In Section 9, the results of investigation are summarized.

2. TWO-BAND MODEL OF INTERACTING FERMIONS

In analysis of the energy structure and the possibility of formation of an excitonic insulator state with the long-range magnetic order, it is convenient to pass to the hole description analogous to that employed in the Emery model [23] that is used in the theory of cuprate superconductors. With account for the aforementioned features of the 5*d* states of the four-valent iridium ions in the octahedral surrounding of oxygen ions, we write the minimal model of $Sr_3Ir_2O_7$ in the hole representation in the following form:

$$\hat{H} = \hat{H}_d + \hat{H}_a + \hat{V}, \tag{1}$$

where operator

$$\hat{H}_d = \sum_f [\xi_d \hat{n}_f + U\hat{n}_{f\uparrow}\hat{n}_{f\downarrow}] + \sum_{ff'\sigma} t_{ff'} d^+_{f\sigma} d_{f'\sigma} \tag{2}$$

describes the subsystem of holes occupying the states on iridium ions. The summation over indices f is performed over the lattice sites at which these ions are located. Fermi operators $d^+_{f\sigma}(d_{f\sigma})$ reflect the creation (annihilation) processes for holes at sites f with spin projection $\sigma = \pm 1/2$, and $\hat{n}_{f\sigma} = d^+_{f\sigma} d_{f\sigma}$ is the operator of the number of holes at site f with spin projection σ. Quantity $\xi_d = \varepsilon_d - \mu$ denotes the hole energy on the iridium ion, which is measured from chemical potential μ. The initial energy of such a hole is denoted by ε_d; U is the Hubbard repulsion energy, and $t_{ff'}$ is the integral of hole hopping between iridium ions locates at sites f and f'. It can easily be seen that operator $\hat{H}_d$ is the Hamiltonian of the Hubbard model [24]. Accordingly, the features of the Fermi states of this subsystem are the same as in the Hubbard model.

The second term of Hamiltonian (1),

$$\hat{H}_a = \sum_{k\sigma} (\varepsilon_k - \mu) a^+_{k\sigma} a_{k\sigma} \quad (3)$$

takes into account the possibility of filling with holes of the subsystem of states appearing as a result of collectivization of oxygen ion orbitals. Each such state characterized by quasi-momentum k and spin projection σ corresponds to energy ε_k. Operator $a^+_{k\sigma}$ ($a_{k\sigma}$) acting on the vector of state leads to the creation (annihilation) of a hole with quasi-momentum k and spin projection σ.

The intersite Coulomb interaction of holes is taken into account by the third term

$$\hat{V} = \sum_{f\delta} V \hat{n}_f \hat{n}_{f+\delta}, \quad (4)$$

in which the number-of-hole operators

$$\hat{n}_f = \sum_\sigma d^+_{f\sigma} d_{f\sigma}, \quad \hat{n}_{f+\delta} = \sum_\sigma a^+_{f+\delta,\sigma} a_{f+\delta,\sigma} \quad (5)$$

correspond to the sites of iridium and oxygen ions, respectively. Operators $a_{f\,+\,\delta,\,\sigma}$ are connected with operators $a_{k\sigma}$ by the conventional Fourier transform. Vector δ connects the site on which an iridium ion is located with the site containing the nearest oxygen ion. Parameter V determines the energy of the intersite Coulomb repulsion of holes locates at such ions.

Considering the experimental data on the realization of the antiferromagnetic ordering in $Sr_3Ir_2O_7$ at low temperatures, as well as the conclusion drawn in [20] concerning the relative decrease in the intensity of fermion hopping between iridium ions under the effect of SOI, we will hereafter consider the minimal model in the regime of strong correlations, when $U \gg |t_{ff'}|$.

It is well known that the use of operators $d_{f\sigma}$ in this case becomes ineffective because it is necessary to take into account the strong interaction rigorously, the operator structure of which is reflected by the product of four operators. This difficulty can be overcome by passing to the atomic representation, in which the Hubbard repulsion operator for fermions on one site acquires the diagonal form. In this case, the hopping operator plays the role of operator of the interaction.

3. EFFECTIVE HAMILTONIAN OF THE MINIMAL MODEL IN THE STRONG CORRELATION REGIME

Going to the atomic representation for the hole subsystem of iridium ions, we note that in the case considered here, the number of such holes per iridium ion does not exceed unity. Since operator $\hat{H}_d$ corresponds to the Hubbard Hamiltonian, we can use the well-known statement that in the Hubbard model corresponds to the t–J model [25–27] in the regime of SEC, in which the Fermi states are described by the lower Hubbard subband.

The effective Hamiltonian obtained using the operator form of perturbation theory [28, 30] can be written in the form

$$H_{\text{eff}} = H_0 + \hat{T} + \hat{J} + \hat{V}, \quad (6)$$

where operator

$$H_0 = \sum_{f\sigma} (\varepsilon_d - \mu) X^{\sigma\sigma}_f + \sum_{k\sigma} (\varepsilon_{ak} - \mu) a^+_{k\sigma} a_{k\sigma} \quad (7)$$

describes noninteracting Hubbard fermions and the aforementioned collectivized fermions that can propagate over the states of oxygen ions.

Here and below, we use the Hubbard operators [31]

$$X^{\sigma\sigma}_f, X^{0\sigma}_f, X^{\sigma 0}_f, X^{\sigma\bar{\sigma}}_f, \quad \bar{\sigma} = -\sigma, \quad (8)$$

acting in the Hilbert subspace of states of the site f. Nondiagonal Fermi-type operator $X^{0\sigma}_f$ describes a transition of the ion on site f from the one-hole state with spin projection σ to the state without a hole. The inverse process is described by the Hermitian conjugate operator $X^{\sigma 0}_f$.

Diagonal Hubbard operator $X^{\sigma\sigma}_f$ projects on the one-hole state with spin projection σ at site f, while X^{00}_f projects onto a state free of hole at the same site. For these operators, the completeness criterion $X^{\sigma\sigma}_f + X^{\bar{\sigma}\bar{\sigma}}_f + X^{00}_f = 1$ is satisfied.

Operator

$$\hat{T} = \sum_{ff'\sigma} t_{ff'} X^{\sigma 0}_f X^{0\sigma}_{f'} \quad (9)$$

corresponds to the inclusion of Hubbard fermion hopping between iridium ions. It should be noted that in view of complicated commutation relations between the Hubbard operators in the subsystem of fermions occupying the electron states on iridium ions, the kinematic interaction is realized [32–34].

The additional interaction appearing between Hubbard fermions located on different iridium ions, which appears in the second order in smallness parameter $t_{ff'}/U$, is described by operator

$$\hat{J} = \frac{1}{2} \sum_{ff'\sigma} J_{ff'} \left(\vec{S}_f \vec{S}_{f'} - \frac{1}{4} \hat{n}_f \hat{n}_{f'} \right), \quad (10)$$

where the exchange interaction intensity is defined by conventional expression

$$J_{ff'} = 2 \frac{|t_{ff'}|^2}{U}.$$

It can easily be seen from the structure of operator $\hat{J}$ that it initiates a transition of the system to the phase with the long-range AFM ordering.

The term of effective Hamiltonian $\hat{V}$ is determined by the same expression (4) with the only difference that the operator of the number of fermions on an iridium ion in the atomic representation has a different form,

$$\hat{n}_f = \sum_{\sigma} X_f^{\sigma\sigma}. \tag{11}$$

4. QUASI-SPIN GREEN'S FUNCTIONS, MAGNON SPECTRUM, AND SUBLATTICE MAGNETIZATION

A distinguishing feature in the model considered here is associated with the fact that the exchange interaction is realized in the subsystem of strongly correlated Hubbard fermions that participate in charge transport as well as in the dynamics of the spin subsystem. It should be expected due to interrelation between the charge and spin degrees of freedom that the details of the electron structure of the two bands affect the characteristics of the magnetic subsystem (e.g., the sublattice magnetization). The inverse effect due to the influence of the AFM ordering on the Fermi excitation spectrum also exists. This means that the problem of the sublattice magnetization must be solved simultaneously with the determination of the characteristics of the fermionic subsystems. The corresponding equations will be considered in the next section.

Before passing to the direct derivation of the equation for the sublattice magnetization, which appears in the complete system of integral self-consistence equations, it should be noted that the spin dynamics is mainly determined by low-energy excitations such as antiferromagnetic magnons. Accordingly, for describing the magnetic subsystem, it is necessary to use the Hubbard operators corresponding to spin degrees of freedom.

For calculating the magnetic excitation spectrum and the sublattice magnetization in the AFM phase, we can use the method of two-time temperature Green's functions [28–30]. The dynamic variables in these GFs are the Hubbard operators corresponding to single-ion transitions without a change in the number of fermions, but with a change in the spin state. This specific feature manifests itself in kinematic relations in the derivation of the motion equations for GFs as well as in the dynamics.

With account for the above arguments, we analyze the dynamic, spectral, and thermodynamic characteristics of the subsystem of the spin degrees of freedom of an exciton antiferromagnet using quasi-spin GFs, which can be written in the quasi-momentum representation in form

$$\begin{aligned} G_{11}(k,\omega) &= \langle\langle S_k^+ \mid S_k^-\rangle\rangle, \\ G_{21}(k,\omega) &= \langle\langle S_{k-Q}^+ \mid S_k^-\rangle\rangle. \end{aligned} \tag{12}$$

Operator S_k^+ is connected with the Hubbard operator $X_f^{\uparrow\downarrow}$ by the Fourier transform:

$$S_k^+ = \frac{1}{\sqrt{N}}\sum_f \exp(-ikf) X_f^{\uparrow\downarrow}. \tag{13}$$

In this case, $S_k^- = (S_k^+)^+$.

Operator $X_f^{\uparrow\downarrow}$ acting on the state at a site with number f and a spin projection of $-1/2$ transforms it into a state with a spin projection of $+1/2$.

The equations of motion for the FGs introduced above, which have been obtained using the Zwanzig–Mori projection technique [35, 36] can be written as

$$\begin{aligned} (\omega - \Sigma_{11}^{(M)}(k))G_{11}(k,\omega) &= \Sigma_{12}^{(M)}(k)G_{21}(k,\omega), \\ (\omega - \Sigma_{22}^{(M)}(k))G_{21}(k,\omega) &= 4M^2 + \Sigma_{21}^{(M)}(k)G_{11}(k,\omega), \end{aligned} \tag{14}$$

where superscript M in mass operator components $\Sigma_{11}^{(M)}(k)$ is used to distinguish them from the mass operator components for fermion GFs that will be used in further analysis. The calculation of these components leads to expressions

$$\begin{aligned} \Sigma_{11}^{(M)}(k) &= \Sigma_{11}^{(T)}(k), \\ \Sigma_{22}^{(M)}(k) &= \Sigma_{22}^{(T)}(k), \\ \Sigma_{12}^{(M)}(k) &= 2M(J_{k-Q} - J_Q) + \Sigma_{12}^{(T)}(k), \\ \Sigma_{21}^{(M)}(k) &= 2M(J_k - J_Q) + \Sigma_{21}^{(T)}(k), \end{aligned} \tag{15}$$

in which $\Sigma_{ij}^T(k)$ are determined by the contributions associated with the hopping of Hubbard fermions over the lattice sites,

$$\begin{aligned} \Sigma_{11}^T(k) &= \frac{1}{2MN}\sum_q [t_{k+q-Q} - t_{q-Q} - t_{k-q} + t_q] L_q(Q), \\ \Sigma_{22}^T(k) &= \frac{1}{2MN}\sum_q [t_{k+q} + t_q - t_{k-q-Q} - t_{q+Q}] L_q(-Q), \\ \Sigma_{12}^T(k) &= \frac{1}{2MN}\sum_q (t_{k+q} + t_{k-q} - 2t_q)\langle N_q\rangle, \\ \Sigma_{21}^T(k) &= \frac{1}{2MN}\sum_q (t_{k-Q+q} + t_{k-Q-q} - 2t_q)\langle N_q\rangle. \end{aligned} \tag{16}$$

The thermodynamic averages appearing in these expressions have the form

$$\begin{aligned} L_q(Q) &= \langle X_{q+Q,\uparrow}^+ X_{q,\uparrow}\rangle, \\ N_q &= \langle X_{q,\uparrow}^+ X_{q,\uparrow}\rangle. \end{aligned} \tag{17}$$

From system (14), we obtain the sought GFs:

$$G_{11}(k,\omega) = \frac{2M\Sigma_{12}^{(M)}(k)}{\det(k,\omega)}, \tag{18}$$

$$G_{12}(k,\omega) = \frac{2M[2M\omega - \Sigma_{11}^{(M)}(k)]}{\det(k,\omega)}, \quad (19)$$

where

$$\det(k,\omega) = [\omega - \Sigma_{11}^{(M)}][\omega - \Sigma_{22}^{(M)}] - \Sigma_{12}^{(M)}\Sigma_{21}^{(M)}. \quad (20)$$

In this expression, the dependence of the mass operator component on the quasi-momentum is not indicated for brevity.

Using the spectral theorem, we can obtain from the resulting expressions the equation for calculating sublattice magnetization

$$M(T) = \frac{n_d}{2\beta(T)}, \quad (21)$$

in which it is convenient to write quantity $\beta(T)$ in the form

$$\beta(T) = \beta_0 + \beta_T. \quad (22)$$

The first term

$$\beta_0 = \frac{1}{N}\sum_q r_q, \quad (23)$$

in which

$$r_q = \frac{\Sigma_{12}^{(M)}(q) + d_q}{\nu_q}, \qquad d_q = \frac{\Sigma_{22}^{(M)}(q) - \Sigma_{11}(q)}{2}, \quad (24)$$

defines the decrease in the sublattice magnetization at zero temperature due to the quantum fluctuations. The second term is associated with the influence of temperature has the form

$$\beta_T = \frac{1}{N}\sum_q \{(r_q + 1)f_B(\Omega_q^+/T) + (r_q - 1)f_B(\Omega_q^-/T)\}.$$

The two branches of the antiferromagnetic magnon spectrum, which appear in this expression, are defined as

$$\Omega_q^{\pm} = \nu_q \pm (\Sigma_{11}^{(M)}(q) + \Sigma_{22}^{(M)}(q))/2, \quad (25)$$

$$\nu_q = \{(d_q)^2 + \Sigma_{12}^{(M)}(q)\Sigma_{21}^{(M)}(q)\}^{(1/2)}, \quad (26)$$

while

$$f_B(x) = \{\exp(x) - 1\}^{-1}$$

is the Bose–Einstein distribution function.

In the limiting case of the conventional dielectric state, when the conduction band and the valence band do not overlap, the contributions associated with hopping vanish. Then $\Sigma_{11}^{(M)} = 0$, $\Sigma_{22}^{(M)} = 0$, and $\Sigma_{12}^{(M)}$ and $\Sigma_{21}^{(M)}$ are determined by the exchange interaction alone:

$$\Sigma_{12}^{(M)}(q) = 2M(J_0 - J_q), \qquad \Sigma_{21}^{(M)}(q) = 2M(J_0 + J_q), \quad (27)$$

where J_q is expressed conventionally in terms of constants $J(h)$ determining the intensities of exchange interactions between the spins at the sites associated with vector h,

$$J_q = \sum_h J(h)\exp(iqh). \quad (28)$$

In this case, we have

$$\beta_0 = \frac{1}{N}\sum_q \frac{J_0 - J_q}{\sqrt{J_0^2 - J_q^2}}. \quad (29)$$

In the approximation of z nearest neighbors, we obtain

$$\beta_0 = \frac{1}{N}\sum_q \frac{1 - \gamma_q}{\sqrt{1 - \gamma_g^2}}, \quad \gamma_q = \frac{1}{z}\sum_h \exp(iqh). \quad (30)$$

In particular, for the square lattice, we obtain the familiar result $\beta_0 = 1.32$. The value of the magnetization reduced by quantum fluctuations is $M = 0.33$.

Equation (21) for the sublattice magnetization appears in the system of self-consistent equations determining the phase of the antiferromagnetic excitonic insulator.

5. GREEN FUNCTIONS OF THE FERMION SUBSYSTEM AND ORDER PARAMETER COMPONENTS OF AN EXCITONIC INSULATOR WITH ANTIFERROMAGNETIC ORDERING

We derive the self-consistent equations describing the phase with the antiferromagnetic ordering with a nonzero EOP using the Green functions constructed on the Hubbard operators of the quasifermionic type.

Taking into account the two-band nature of the system and the existence of the AFM order, we introduce the four-component operator of the Fermi type:

$$\hat{\Psi}_{k\sigma} = (X_{k\sigma}, a_{k\sigma}, X_{k-Q,\sigma}, a_{k-Q,\sigma}). \quad (31)$$

Here, $X_{k\sigma}$ corresponds to operators $X_f^{0\sigma}$ and is connected with them via the Fourier transform:

$$X_f^{0\sigma} = \frac{1}{\sqrt{N}}\sum_k e^{ikf} X_{k\sigma}. \quad (32)$$

An analogous relation is also observed for operator $X_{k-Q,\sigma}$ if we perform in it the obvious renormalization for quasi-momentum, $k \to k - Q$.

The introduction of vector Q is required because of the necessity of taking into account the aforementioned antiferromagnetic ordering in the Hubbard fermion subsystem:

$$\langle S_f^z \rangle = \frac{1}{2}\langle X_f^{\uparrow\uparrow} - X_f^{\downarrow\downarrow} \rangle = M \exp(iQf), \quad (33)$$

where amplitude M corresponds to the magnetization of the antiferromagnetic sublattice. In the 2D case, we have $Q = (\pi, \pi)$, while for the 3D structure, we assume that $Q = (\pi, \pi, \pi)$.

Using four-component operators (31), we define the matrix Green function

$$\hat{G}^\sigma(k, t - t') = -i\theta(t - t')\langle\{\hat{\Psi}_{k\sigma}(t), \hat{\Psi}^+_{k\sigma}(t')\}_+\rangle, \quad (34)$$

which will allow us to describe the spectral and thermodynamic characteristics of the subsystem of Fermi degrees of freedom of the antiferromagnetic ED.

As usual, $\hat{\Psi}_{k\sigma}(t)$ in expression (34) is an operator in the Heisenberg representation, taken at instant t, and $\hat{\Psi}^+_{k\sigma}(t')$ is the Hermitian conjugate operator at instant t'; $\theta(t - t')$ is the unit Heaviside function. The angle brackets indicate that anticommutator $\{\hat{\Psi}_{k\sigma}(t), \hat{\Psi}^+_{k\sigma}(t')\}_+$ contained in them is subjected to statistical averaging.

Using the Zwanzig–Mori projection technique [35, 36] for operators appearing after the commutation $[\hat{\Psi}_{k\sigma}, \hat{H}]_-$, we find that the system of equations for the Fourier transform of the GF is defined by integral transformation

$$\hat{G}^\sigma(k, t) = \frac{1}{2\pi}\int d\omega \exp(-i\omega t)\hat{G}^\sigma(k, \omega), \quad (35)$$

can be written in concise form as matrix equation

$$[\omega\hat{I} - \hat{\Sigma}^\sigma(k)]\hat{G}^\sigma(k, \omega) = \hat{S}^\sigma. \quad (36)$$

Here, $\hat{I}$ is the 4×4 unit matrix and $\hat{S}$ is the matrix, the elements of which are the mean values of the anticommutators of the components of operators $\hat{\Psi}_{k\sigma}$ and $\hat{\Psi}^+_{k\sigma}$:

$$(\hat{S}^\sigma)_{ij} = \langle\{\hat{\Psi}_{i;k\sigma}, \hat{\Psi}^+_{j;k\sigma}\}_+\rangle. \quad (37)$$

It should be emphasized that in the phase with AFM ordering, matrix $\hat{S}$ contains nonzero nondiagonal elements and has the form

$$\hat{S}^\sigma = \begin{pmatrix} 1 - n_d/2 & 0 & \eta_\sigma M & 0 \\ 0 & 1 & 0 & 0 \\ \eta_\sigma M & 0 & 1 - n_d/2 & 0 \\ 0 & 0 & 0 & 1 \end{pmatrix},$$

where

$$n_d = \frac{1}{N}\sum_{k\sigma}\langle X^+_{k\sigma}X_{k\sigma}\rangle \quad (38)$$

denotes the average number of the Hubbard fermions per unit cell and M is the sublattice magnetization defined in expression (33). Function η_σ depending on the spin projection is defined as

$$\eta_\sigma = 2\sigma, \quad \sigma = \pm(1/2). \quad (39)$$

The nondiagonal form of matrix $\hat{S}$, which is a consequence of the nonorthogonality of the system of basis operators (31), substantially affects the form of the coefficients in the equations of motion for GFs. The account for this circumstance ensures the required analytical properties of these functions.

Matrix $\hat{\Sigma}^\sigma(k)$ appearing in expression (36) is determined from the expression

$$\hat{\Sigma}^\sigma(k) = \hat{D}^\sigma(k)[\hat{S}^\sigma]^{-1}, \quad (40)$$

in which the elements of dynamical matrix $\hat{D}(k)$ are calculated in terms of the average value of anticommutator $[\hat{\Psi}_{i;k\sigma}, \hat{H}]_-$ with operators appearing in $\hat{\Psi}^+_{j;k\sigma}$,

$$\hat{D}^\sigma_{ij}(k) = \langle\{[\hat{\Psi}_{i;k\sigma}, \hat{H}]_-, \hat{\Psi}^+_{j;k\sigma}\}_+\rangle. \quad (41)$$

Subscripts i and j run through the values from 1 to 4, and $\hat{\Psi}^+_{j;k\sigma}$ is the operator Hermitian conjugate to the jth operator in expression (31).

Without dwelling onto details of simple but cumbersome calculations, we write the final result:

$$\hat{\Sigma}^\sigma(k) = \begin{pmatrix} \varepsilon_{dk} & \Delta^\sigma_{21}(k) & u_{\sigma kQ} & \Delta^\sigma_{41}(k) \\ \Sigma^\sigma_{21}(k) & \varepsilon_{ak} & \Sigma^\sigma_{23}(k) & 0 \\ u_{\sigma k} & \Delta^\sigma_{23}(k) & \varepsilon_{dkQ} & \Delta^\sigma_{43}(k) \\ \Sigma^\sigma_{41}(k) & 0 & \Sigma^\sigma_{43}(k) & \varepsilon_{akQ} \end{pmatrix},$$

where the following notation is used for energy quantities:

$$\varepsilon_{dk} = \varepsilon_d + (1 - n_d/2)t_{dk}, \quad u_{\sigma k} = \eta_\sigma M(J_Q + t_{dk}), \quad (42)$$

$$\varepsilon_{dkQ} = \varepsilon_d + (1 - n_d/2)t_{dkQ}, \quad t_{dkQ} = t_{d,k-Q}, \quad (43)$$

$$u_{\sigma kQ} = \eta_\sigma M(J_Q + t_{dkQ}), \quad \varepsilon_{akQ} = \varepsilon_{d,k-Q}. \quad (44)$$

The EOPs are defined as

$$\begin{aligned} \Delta^\sigma_{21}(k) &= -\frac{1}{N}\sum_q V_{k-q}\langle a^+_{q\sigma}X_{q\sigma}\rangle, \\ \Delta^\sigma_{41}(k) &= -\frac{1}{N}\sum_q V_{k-q}\langle a^+_{q-Q,\sigma}X_{q\sigma}\rangle, \\ \Delta^\sigma_{23}(k) &= -\frac{1}{N}\sum_q V_{k-q}\langle a^+_{q\sigma}X_{q-Q\sigma}\rangle, \\ \Delta^\sigma_{43}(k) &= -\frac{1}{N}\sum_q V_{k-q}\langle a^+_{q-Q\sigma}X_{q-Q\sigma}\rangle. \end{aligned} \quad (45)$$

These expressions show that the EOP components can be represented as superpositions of mean values of the product of Hubbard fermions with traditional fermions. This determines the specific feature of the formation of the exciton phase in a strongly correlated system because the on-site Coulomb interaction leads to the splitting of the upper Hubbard subband. As a result, the charge carrier dynamics is determined only by fermions of the lower Hubbard subband. This means that the exciton pairing occurs between strongly correlated fermions and conventional fermions, and the pairing intensity is proportional to the intersite Coulomb interaction. The EOP definition implies that $\Delta_{ij}^{\sigma}(k) = (\Delta_{ji}^{\sigma}(k))^*$.

The matrix elements can be expressed in terms of the EOP components introduced above:

$$\begin{aligned}
\Sigma_{21}^{\sigma}(k) &= [(1 - n_d/2)\Delta_{12}^{\sigma}(k) - \eta_{\sigma} M \Delta_{32}^{\sigma}(k)]/L,\\
\Sigma_{23}^{\sigma}(k) &= [(1 - n_d/2)\Delta_{32}^{\sigma}(k) - \eta_{\sigma} M \Delta_{12}^{\sigma}(k)]/L,\\
\Sigma_{41}^{\sigma}(k) &= [(1 - n_d/2)\Delta_{14}^{\sigma}(k) - \eta_{\sigma} M \Delta_{34}^{\sigma}(k)]/L,\\
\Sigma_{43}^{\sigma}(k) &= [(1 - n_d/2)\Delta_{34}^{\sigma}(k) - \eta_{\sigma} M \Delta_{14}^{\sigma}(k)]/L,
\end{aligned} \tag{46}$$

where quantity L is the determinant of matrix $\hat{S}^{\sigma}$:

$$L = (1 - n_d/2)^2 - M^2. \tag{47}$$

6. SELF-CONSISTENT EQUATIONS FOR AN EXCITON ANTIFERROMAGNET

Definitions (45) show that the derivation of the self-consistent equation for EOP components in explicit form involves the calculation of the mean values of the product of the Fermi operators as well as the operators corresponding to the Hubbard fermions. These mean values are determined using the spectral theorem [28, 29] with corresponding GFs. In particular,

$$\langle a_{q\sigma}^{+} X_{q\sigma}\rangle = \int \frac{d\omega}{e^{\beta\omega}+1}\left[-\frac{1}{\pi}\operatorname{Im} G_{12}^{\sigma}(q,\omega + i\delta)\right], \tag{48}$$

$$\langle a_{q\sigma}^{+} X_{q-Q\sigma}\rangle = \int \frac{d\omega}{e^{\beta\omega}+1}\left[-\frac{1}{\pi}\operatorname{Im} G_{32}^{\sigma}(q,\omega + i\delta)\right], \tag{49}$$

where $\beta = 1/T$, T being the temperature of the system, and $\delta \to +0$.

Analogously, mean values $\langle a_{q-Q\sigma}^{+} X_{q\sigma}\rangle$ and $\langle a_{q-Q\sigma}^{+} X_{q-Q\sigma}\rangle$ are calculated, the only difference being that subscripts "12" and "32" on the matrix elements of the GF must be replaced by "14" and "34," respectively.

The substitution of the resulting mean values into expressions (45) leads to the integral self-consistent equations for the EOP components. Analysis shows that the AFM phase of EI is realized for nonzero components $\Delta_{21}^{\sigma}(k)$ and $\Delta_{23}^{\sigma}(k)$, while the two other components $\Delta_{41}^{\sigma}(k)$ and $\Delta_{43}^{\sigma}(k)$ are equal to zero. This is due to the fact that the singularities in the denominators in the integrands for these components, which are due to the closeness of the energies of the second and third branches of the Fermi excitation spectrum at the center and edges of the Brillouin zone, are compensated by the factors appearing in the numerators of these expressions. For this reason, the fermion pairing condition ensuring the finiteness of parameters Δ_{41} and $\Delta_{43}^{\sigma}(k)$ becomes unsatisfiable.

On account for these arguments, we find that matrix $\hat{\Sigma}^{\sigma}(k)$ takes a simpler form, and the GFs required for the derivation of the self-consistent equations are defined as

$$G_{12}^{\sigma}(k,\omega) = \frac{(\omega - \varepsilon_{dkQ})\Delta_{21}^{\sigma}(k) + u_{\sigma kQ}\Delta_{23}^{\sigma}(k)}{\det_3(k,\omega)}, \tag{50}$$

$$G_{32}^{\sigma}(k,\omega) = \frac{(\omega - \varepsilon_{dk})\Delta_{23}^{\sigma}(k) + u_{\sigma k}\Delta_{21}^{\sigma}(k)}{\det_3(k,\omega)}, \tag{51}$$

where $\det_3(k, \omega)$ is the third-order determinant composed of the elements of matrix $\hat{\Sigma}^{\sigma}(k)$, which has form

$$\begin{aligned}
\det_3(k,\omega) &= (\omega - \varepsilon_{dk})(\omega - \varepsilon_{ak})(\omega - \varepsilon_{dkQ})\\
&- (\omega - \varepsilon_{dk})\Delta_{23}^{\sigma}\Sigma_{23}^{\sigma} - (\omega - \varepsilon_{dkQ})\Delta_{21}^{\sigma}\Sigma_{21}^{\sigma}\\
&- (\omega - \varepsilon_{ak})u_{\sigma k}u_{\sigma kQ} - u_{\sigma k}\Delta_{21}^{\sigma}\Sigma_{23}^{\sigma} - u_{\sigma kQ}\Delta_{23}^{\sigma}\Sigma_{21}^{\sigma}.
\end{aligned} \tag{52}$$

In this expression, the indication of the dependence of quantities $\Delta_{ij}^{\sigma}(k)$ and $\Sigma_{ij}^{\sigma}(k)$ on the quasimomentum has been omitted for brevity.

The application of the spectral theorem leads to two self-consistent integral equations:

$$\begin{aligned}
\Delta_{21}^{\sigma}(k) &= \frac{-1}{N}\sum_{q} V_{k-q}[\Phi_{3q}\Delta_{21}^{\sigma}(q) + u_{\sigma qQ}F_q\Delta_{23}^{\sigma}(q)],\\
\Delta_{23}^{\sigma}(k) &= \frac{-1}{N}\sum_{q} V_{k-q}[\Phi_{1q}\Delta_{23}^{\sigma}(q) + u_{\sigma q}F_q\Delta_{21}^{\sigma}(q)].
\end{aligned} \tag{53}$$

In these equations, three functions are used, in terms of which the temperature dependences of the EOP components and other thermodynamic quantities are manifested.

First function F_q is defined in terms of the sum of three addends,

$$F_q = \sum_{i=1}^{3}\varphi_{iq}, \tag{54}$$

each of which is connected with the Fermi–Dirac distribution function and the combinations of the energy differences for three branches of the Fermi spectrum:

$$\varphi_{1q} = \frac{f[(E_{1q}-\mu)/T]}{(E_{1q}-E_{2q})(E_{1q}-E_{3q})},$$
$$\varphi_{2q} = \frac{f[(E_{2q}-\mu)/T]}{(E_{2q}-E_{1q})(E_{2q}-E_{3q})}, \quad (55)$$
$$\varphi_{3q} = \frac{f[(E_{3q}-\mu)/T]}{(E_{3q}-E_{1q})(E_{3q}-E_{2q})}.$$

Energies E_{1q}, E_{2q}, and E_{3q} can be determined by solving dispersion equation

$$\det_3(q, E_{iq}) = 0, \quad i = 1,2,3, \quad (56)$$

and can be written in the form

$$E_{1q} = -W_q/2 - \lambda_q - a_q/3,$$
$$E_{2q} = -W_q/2 + \lambda_q - a_q/3, \quad (57)$$
$$E_{3q} = W_q - a_q/3.$$

The functions of the quasi-momentum appearing in these expressions,

$$W_q = Z_q - P_q/Z_q, \quad Z_q = (\sqrt{Q_q^2 + P_q^3} - Q_q)^{1/3}, \quad \lambda_q = \sqrt{-3P_q - 3W_q^2/4} \quad (58)$$

are connected with the initial energy quantities by relations

$$P_q = \frac{1}{3}(b_q - a_q^2/3), \quad Q_q = (c_q + 2a_q^3/27 - a_q b_q/3)/2,$$
$$a_q = -(\varepsilon_{aq} + \varepsilon_{dq} + \varepsilon_{dqQ}), \quad (59)$$
$$b_q = \varepsilon_{aq}\varepsilon_{dq} + \varepsilon_{dq}\varepsilon_{dqQ} + \varepsilon_{aq}\varepsilon_{dqQ} - u_{\sigma q}u_{\sigma qQ} - \Delta_{23}\Sigma_{23} - \Delta_{21}\Sigma_{21},$$

$$c_q = -\varepsilon_{aq}\varepsilon_{dq}\varepsilon_{dqQ} + \varepsilon_{aq}u_{\sigma q}u_{\sigma qQ} + \varepsilon_{dq}\Delta_{23}\Sigma_{23} + \varepsilon_{dqQ}\Delta_{21}\Sigma_{21} - u_{\sigma q}\Delta_{21}\Sigma_{23} - u_{\sigma qQ}\Delta_{23}\Sigma_{21}. \quad (60)$$

The other two functions appearing in expression (53) can also be represented as the sum of three terms, each of which contains an additional energy factor:

$$\Phi_{1q} = \sum_{i=1}^{3}(E_{iq} - \varepsilon_{dq})\varphi_{iq},$$
$$\Phi_{3q} = \sum_{i=1}^{3}(E_{iq} - \varepsilon_{dqQ})\varphi_{iq}. \quad (61)$$

These equations imply that the expressions appearing in them depend, apart from the components of EOP and the sublattice magnetization, on concentration n_d of the Hubbard fermions. To derive the equation defining these quantity, we note that the total number of holes per unit-cell in the system considered here is equal to 1. This means that the additional equation determining the position of the chemical potential has the form

$$n_d + n_a = 1. \quad (62)$$

The derivation of the explicit expressions for the quantities appearing in this equation involves the application of the fermionic GFs:

$$G_{11}^{\sigma}(k,\omega) = \frac{(1-n_d/2)a_{11}(k,\omega) + \eta_\sigma M a_{31}(k,\omega)}{\det_3(k,\omega)}, \quad (63)$$

$$G_{22}^{\sigma}(k,\omega) = \frac{(\omega - \varepsilon_{dk})(\omega - \varepsilon_{dkQ}) - u_{\sigma k}u_{\sigma kQ}}{\det_3(k,\omega)}, \quad (64)$$

where

$$a_{11}(k,\omega) = (\omega - \varepsilon_{ak})(\omega - \varepsilon_{dkQ}) - \Sigma_{23}^{\sigma}(k)\Delta_{23}^{\sigma}(k),$$
$$a_{31}(k,\omega) = (\omega - \varepsilon_{ak})u_{\sigma kQ} + \Sigma_{23}^{\sigma}(k)\Delta_{21}^{\sigma}(k). \quad (65)$$

The application of the spectral theorem leads to the sought expressions for n_d and n_a:

$$n_d = \frac{(1-n_d/2)}{N}\sum_{q\sigma}P_d(q) + \frac{M}{N}\sum_{q\sigma}\eta_\sigma R_{d\sigma}(q), \quad (66)$$

$$n_a = \frac{1}{N}\sum_{q\sigma}\sum_{j=1}^{3}U_j(q)\phi_{jq}. \quad (67)$$

Here, we used the following notation:

$$P_d(q) = \sum_{j=1}^{3}a_{11}(q, E_{jq})\varphi_{jq}, \quad (68)$$

$$R_d(q) = \sum_{j=1}^{3}a_{31}(q, E_{jq})\varphi_{jq}, \quad (69)$$

$$U_j(q) = [(E_{jq} - \varepsilon_{dq})(E_{jq} - \varepsilon_{dqQ}) - u_{\sigma q}u_{\sigma qQ}]. \quad (70)$$

Two self-consistent integral equations (53) together with Eqs. (21), (66), and (67) form a closed system describing the domain of realization of the exciton phase with a long-range AFM ordering, as well as the relations between the characteristics of the AFM EI phase and the initial parameters of the model. The specific dependence of the EOP components on the quasi-momentum (symmetry type) is determined by the kernel of the integral equation and the condition of the lowest value of energy of the resulting phase.

7. SYMMETRY CLASSIFICATION OF PHASES

The further analysis of admissible solutions to the aforementioned system of equations will be confined to a 2D lattice. In this case, the point symmetry group has two 1D and two 2D complex-conjugate irreducible representations (IR).

In the nearest neighbor approximation, the basis functions of 1D IRs have form

$$\varphi_s(k) = \cos\frac{k_x}{2}\cos\frac{k_y}{2}, \quad s-\text{symmetry type},$$
$$\varphi_d(k) = \sin\frac{k_x}{2}\sin\frac{k_y}{2}, \quad d-\text{symmetry type}. \quad (71)$$

For a 2D IR, basis function of the p-type symmetry is characterized by a more intricate quasi-momentum dependence [18]:

$$\varphi_{p\sigma}(k) = (\eta_\sigma - i)\sin\frac{k_x}{2}\cos\frac{k_y}{2} + (\eta_\sigma + i)\cos\frac{k_x}{2}\sin\frac{k_y}{2}.$$

Its important property is due to the fact that upon substitution $\sigma \to -\sigma$, we obtain $\varphi_{p\sigma}(k) \to \varphi^*_{p\sigma}(k)$.

The possibility of realization of the solution with such a symmetry type of the order parameter is of special importance because the AFM EI phase is characterized by a nontrivial topology of the energy structure (i.e., corresponds to a topological insulator with a long-range AFM order). The interest in such states has increased significantly after the publications [37–39] indicating the realization of the antiferromagnetic topological insulator state in $MnBi_2Te_4$.

Let us expand the Coulomb interaction potential

$$V_{k-q} = 4V\cos\frac{(k_x - q_x)}{2}\cos\frac{(k_y - q_y)}{2} \tag{72}$$

appearing in the kernel of the integral equation for the Fourier transform in the IR functions:

$$\begin{aligned} V_{k-q} = V[&4\varphi_s(k)\varphi_s(k) + 4\varphi_d(k)\varphi_d(q) \\ &+ \varphi^*_{pq}(k)\varphi_{pq}(q) + \varphi_{p\sigma}(k)\varphi^*_{pq}(q)]. \end{aligned} \tag{73}$$

Since the IR basis functions are orthogonal to one another, we can perform the classification of solutions to system (53) in accordance with the three aforementioned symmetry types. In this case, the quasi-momentum dependences of EOP for each symmetry type can be written in unified form:

$$\begin{aligned} \Delta^\sigma_{21}(k) &= \Delta_{\nu 1}\varphi_\nu(k), \\ \Delta^\sigma_{23}(k) &= \eta_\sigma\Delta_{\nu 2}\varphi_\nu(k), \end{aligned} \tag{74}$$

where subscript ν takes one of three values s, d, or p.

We pay attention to the fact that $\Delta^\sigma_{21}(k)$ for the s- and d-symmetry types is independent of the spin projection, while $\Delta^\sigma_{23}(k)$ reverses its sign upon a change in the value of σ to the opposite value. The situation for the p-symmetry type is more complicated because, as noted above, the basis function itself for this symmetry type depends on the spin. Nevertheless, after the parameterization of amplitudes, the dependence of these quantities on the spin projection disappears. It should be emphasized that this had become possible owing to the inclusion of the explicit dependence of quantities $u_{\sigma k} = \eta_\sigma M(J_Q + t_{dk})$ and $u_{\sigma k} = \eta_\sigma M(J_Q + t_{dkQ})$ on the spin projection leading to the sign reversal upon the substitution $\sigma \to -\sigma$.

Substituting these expressions into (53), we obtain a system of two transcendental equations for order parameter amplitudes $\Delta_{\nu 1}$ and $\Delta_{\nu 2}$:

$$\begin{aligned} (1 + A_{\nu 3})\Delta_{\nu 1} + MB_{\nu 3}\Delta_{\nu 2} &= 0, \\ MB_{\nu 1}\Delta_{\nu 1} + (1 + A_{\nu 1})\Delta_{\nu 2} &= 0. \end{aligned} \tag{75}$$

Here, the following notation are used:

$$A_{\nu 1} = \frac{V}{N}\sum_q \Gamma_{\nu q}\Phi_{1q}, \quad A_{\nu 3} = \frac{V}{N}\sum_q \Gamma_{\nu q}\Phi_{3q}, \tag{76}$$

$$B_{\nu 1} = \frac{V}{N}\sum_q \Gamma_{\nu q}(J_Q + t_{dq})F_q, \tag{77}$$

$$B_{\nu 3} = \frac{V}{N}\sum_q \Gamma_{\nu q}(J_Q + t_{dqQ})F_q. \tag{78}$$

Depending on the type of representation, function $\Gamma_{\nu q}$ can be written as

$$\begin{aligned} \Gamma_{sq} &= (1+\cos q_x)(1+\cos q_y), \quad s\text{–symmetry type}, \\ \Gamma_{dq} &= (1-\cos q_x)(1-\cos q_y), \quad d\text{–symmetry type}, \\ \Gamma_{dq} &= 1 - \cos q_x \cos q_y, \quad p\text{–symmetry type}. \end{aligned} \tag{79}$$

It follows from system (75) that the existence of the long-range AFM ordering leads to binding of amplitudes Δ^0_{21} and Δ^0_{23}. For $M = 0$, the condition of the realization of the excitonic insulator phase is expressed by equation

$$1 + A_3 = 0, \tag{80}$$

which describes the phase when the excitonic pairing occurs between the Hubbard fermions of the lower band and conventional fermions of the upper band.

8. ANTIFERROMAGNETIC EI WITH s-TYPE ORDER PARAMETER SYMMETRY

The state with the highest value of the condensation energy corresponds to the solution to the system of equations with the s-type EOP symmetry. Figure 1 shows a typical energy spectrum of the Fermi states in the AFM phase of EI.

The existence of the AFM ordering without taking into account exciton pairing leads to the emergence of two branches of the Hubbard fermion spectrum. The quasi-momentum dependences of these branches are connected genetically with the quasi-momentum dependences described by functions ε_{dk} and ε_{dkQ}. Since ε_{dkQ} can be obtained from ε_{dk} by shifting through antiferromagnetism vector Q, there exist the values of quasi-momenta, at which these functions have identical values. At these points, the effect of the long-range magnetic order via the mechanism of exchange interaction between the Hubbard fermions is the strongest. As a result, "repulsion" of the branches occurs, and the two-band structure of the Hubbard fermion spectrum, which is initiated by the AFM ordering, appears in the subsystem of the same fermions.

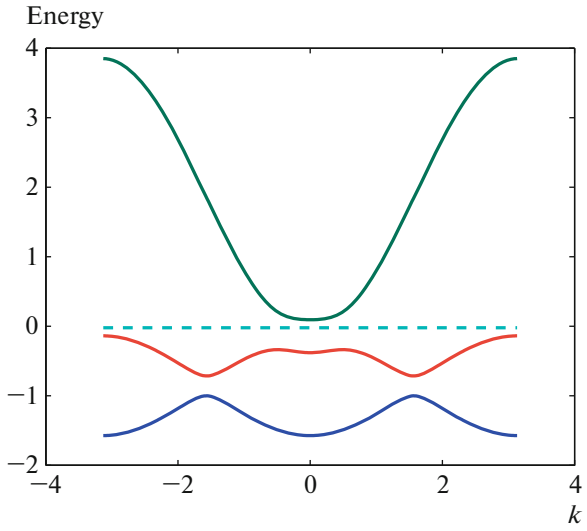

Fig. 1. Fermi excitation spectrum of an antiferromagnetic excitonic insulator. The quasi-momentum along the principal diagonal of the Brillouin zone is laid along the abscissa axis. The energy in electronvolts is laid along the ordinate axis. The lower blue curve corresponds to energy E_{1k}; the middle red curve corresponds to E_{2k}, and the upper green curve, to E_{3k}. Calculations are performed in the nearest neighbor approximation for parameters $t_{b1} = 0.5$, $t_{a1} = -0{,}5$, $\Delta_0 = 0.3$, $V = 1$, and $U = 5$. The solution of the system of self-consistent equations has led to the following values of quantities: Hubbard fermion concentration $n_d = 0.994$; the exciton order parameter components are $\Delta^0_{12} = -0.145$, $\Delta^0_{23} = -0.043$, $\Delta^0_{34} = 0$, and $\Delta^0_{14} = 0$. Dashed line shows the position of chemical potential $\mu = -0.022$.

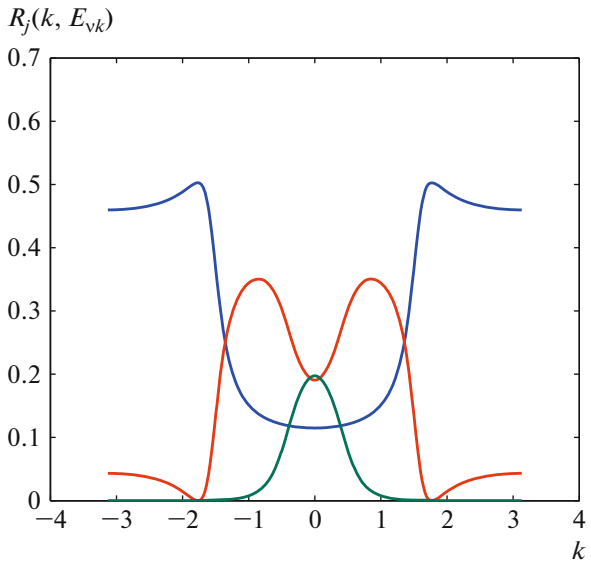

Fig. 2. Behavior of functions $R^\sigma_j(k, E_{\nu k})$ along the direction of the principal diagonal of the Brillouin zone. All energy parameters are the same as in Fig. 1. The blue curve describes the behavior of $R^\sigma_1(k, E_{1k})$; the red curve corresponds to quasi-momentum dependence $R^\sigma_2(k, E_{2k})$; the green curve shows dependence $R^\sigma_3(k, E_{3k})$.

To clarify the reason for zero values of $\Delta^\sigma_{41}(k)$ and $\Delta^\sigma_{41}(k)$ in the AFM phase of EI, we consider the spectral intensity (SI) $A^\sigma(k, \omega)$ associated with the correlation function of the Hubbard fermions $\langle X^+_{k\sigma}(t')X_{k\sigma}(t)\rangle$ in terms of the Fourier transform:

$$\langle X^+_{k\sigma}(t')X_{k\sigma}(t)\rangle = \int \frac{d\omega}{2\pi}\exp\{-i\omega(t-t')\}A^\sigma(k,\omega). \tag{81}$$

Using the well-known expression [28, 29]

$$A^\sigma(k,\omega) = -\frac{1}{\pi}\operatorname{Im} G^\sigma(k,\omega+i\delta), \tag{82}$$

we write SI in the form

$$A^\sigma(k,\omega) = \sum_{\nu=1}^{3} R^\sigma_\nu(k, E_{\nu k})\delta(\omega - E_{\nu k}). \tag{83}$$

Quantities $R^\sigma_\nu(k, E_{\nu k})$ appearing in this representation and determining the weight contribution to SI associated with the fermion branch with number ν at each point of the Brillouin zone are defined as

$$\begin{aligned} R^\sigma_1(k, E_{1k}) &= \frac{g_{11}(k, E_{1k})}{\lambda_k(3W_k + 2\lambda_k)}, \\ R^\sigma_2(k, E_{2k}) &= \frac{g_{11}(k, E_{2k})}{\lambda_k(2\lambda_k - 3W_k)}, \\ R^\sigma_3(k, E_{3k}) &= \frac{g_{11}(k, E_{3k})}{(3W_k - 2\lambda_k)(3W_k + 2\lambda_k)}, \end{aligned} \tag{84}$$

where

$$\begin{aligned} &g_{11}(k, E_{\nu k}) \\ &= (1 - n_d/2)a_{11}(k, E_{\nu k}) + \eta_\sigma M a_{31}(k, E_{\nu k}). \end{aligned} \tag{85}$$

Functions $a_{11}(k, \omega)$ and $a_{31}(k, \omega)$ appearing in these expressions are defined in (65), while quantities λ_k and W_k have been introduced in writing the solutions to the cubic equation.

Figure 2 shows the quasi-momentum dependences $R^\sigma_\nu(k, E_{\nu k})$ in the direction of the principal diagonal. It can be seen that near the Brillouin zone center, there exists a large region in which all functions $R^\sigma_\nu(k, E_{\nu k})$ differ from zero. In the conditions when all the initial bands overlap, this circumstance is responsible for the existence of a solution with $\Delta^\sigma_{21}(k) \neq 0$ and $\Delta^\sigma_{23}(k) \neq 0$.

Let us consider in greater detail the quantitative analysis of the reason for zero values of components $\Delta^\sigma_{41}(k)$ and $\Delta^\sigma_{43}(k)$ in the AFM EI in question. It should

be noted above all that the emergence of correlations ensuring nonzero values of these components is associated with the fermions of the upper branch that is genetically initiated in initial spectrum ε_{akQ} and is modified self-consistently. However, this requires the fulfillment of two conditions. First, the energy difference between the branches, for which the formation of a relation between fermions is expected, must be small. Second, the system must contain fermions that participate in the formation of the bond. Analytically, this is expressed in the condition for the existence of a region in the Brillouin zone, in which two quantities $R^{\sigma}_{\nu_1}(k,\ E_{\nu_1 k})$ and $R^{\sigma}_{\nu_2}(k,\ E_{\nu_2 k})$ (subscripts ν_1 and ν_2 denote the numbers of the fermion branches, for which the possibility of bond formation is analyzed) differ from zero. The curves in Fig. 2 show that the above conditions cannot be satisfied. This explains the equality to zero of components $\Delta^{\sigma}_{41}(k)$ and $\Delta^{\sigma}_{43}(k)$ in the AFM phase of EI considered here.

9. CONCLUSIONS

Let us formulate the main conclusion drawn from analysis of the joint effect of the spin–orbit interaction and strong electron correlations on the conditions for the existence of an excitonic insulator with the AFM order.

1. The fundamental problem of the realization of AFM EI in iridium oxides can be solved using the minimal two-band model taking into account the peculiarities of the electron structure of these oxides and the strong spin–orbit interaction in ions with the 5*d* electron configuration. The use of the electron–hole symmetry in the system of strongly correlated fermions and taking into account the type of filling of electrons states of oxygen ions has made it possible to pass to the hole description of the two-band model like it is done in the theory of cuprate superconductors.

2. The inclusion of strong electron correlations in the iridium ion subsystem leads to the emergence (in accordance with the Anderson mechanism) of the exchange interaction of the AFM type in the subsystem of the Hubbard fermions filling the states of the lower band. In this case, the intersite Coulomb interaction ensuring spontaneous hybridization of mixing of fermions from different bands plays the role of the mechanism of formation of the excitonic insulator phase with a long-range antiferromagnetic ordering.

3. The AFM ordering is responsible for the emergence of two branches in the Hubbard fermion spectrum. For this reason, the AFM phase of EI is characterized by exciton components $\Delta^{\sigma}_{21}(k)$ and $\Delta^{\sigma}_{23}(k)$ appearing as a result of hybridization of free fermions of the upper band with the Hubbard fermions described by operators $X_{k\sigma}$ and $X_{k-Q,\sigma}$, respectively.

4. For the solutions to the system of self-consistent integral equations, symmetry classification has been performed, in accordance with which the quasi-momentum dependences of the exciton order parameter components can be of the *s*, *p*, or *d* types. The ground state corresponds to the solution with the *s*-type symmetry.

5. Fermi excitations in the AFM phase of EI near the center of the Brillouin zone are formed under the strong influence of the emerging hybridization of the Hubbard fermions with free fermions in the upper band. This hybridization induces a dielectric gap, transforming the system from the semimetal state to the dielectric state with a long-range AFM order.

6. The model formulated here makes it possible to interpret qualitatively the properties of the antiferromagnetic phase of an excitonic insulator, which (as stated in some publications) is realized in compound $Sr_3Ir_2O_7$.

CONFLICT OF INTEREST

The author declares that he has no conflicts of interest.

ADDITIONAL INFORMATION

This article is prepared for the memorial issue of the journal dedicated to the 95th birthday of L.A. Prozorova.

REFERENCES

1. A. S. Borovik-Romanov, in *Antiferromagnetism and Ferrites* (Akad. Nauk SSSR, Moscow, 1962), p. 5 [in Russian].
2. A. V. Chubukov, S. Sachdev, and J. Ye, Phys. Rev. B **49**, 11919 (1994).
3. D. H. Lee, J. D. Joannopoulos, J. W. Negele, et al., Phys. Rev. Lett. **433A**, 52 (1984).
4. H. Kawamura, S. Miyashita, J. W. Negele, et al., Phys. Rev. Lett. **54**, 453952 (1985).
5. A. V. Chubukov and D. I. Golosov, J. Phys.: Condens. Matter **3**, 69 (1991).
6. A. I. Smirnov, Phys. Usp. **59**, 564 (2016).
7. L. E. Svistov, A. I. Smirnov, L. A. Prozorova, O. A. Petrenko, A. Ya. Shapiro, and L. N. Dem'yanets, JETP Lett. **80**, 204 (2004).
8. L. E. Svistov, L. A. Prozorova, A. M. Farutin, A. A. Gippius, K. S. Okhotnikov, A. A. Bush, K. E. Kamentsev, and E. A. Tishchenko, J. Exp. Theor. Phys. **108**, 1000 (2009).
9. L. V. Keldysh and Yu. V. Kopaev, Sov. Phys. Solid State **6**, 2219 (1964).
10. A. N. Kozlov and L. A. Maksimov, Sov. Phys. JETP **21**, 790 (1965).
11. J. de Cloiseaux, J. Phys. Chem. Solids **26**, 259 (1965).
12. Y. Lu, H. Kono, T. Larkin, A. Rost, T. Takayama, A. Boris, B. Keimer, and H. Takagi, Nat. Commun. **8**, 14408 (2017).

13. N. I. Kulikov and V. V. Tugushev, Sov. Phys. Usp. **27**, 954 (1984).
14. D. G. Mazzone, Y. Shen, H. Suwn, et al., Nat. Commun. **26**, 259 (2022).
15. M. Z. Hasan and C. L. Kane, Rev. Mod. Phys. **82**, 3045 (2010).
16. X. L. Qi and S. C. Zhang, Rev. Mod. Phys. **83**, 1057 (2011).
17. L. Balents, Nature (London, U.K.) **464**, 199 (2010).
18. V. V. Val'kov, JETP Lett. **111**, 647 (2020).
19. B. J. Kim, Hosub Jin, S. J. Moon, et al., Phys. Rev. Lett. **101**, 076402 (2008).
20. J.-M. Carter, V. Vijay Shankar, and Hae-Young Kee, Phys. Rev. B **86**, 035111 (2013).
21. R. Schaffer, E. Kin-Ho Lee, B.-J. Yang, et al., Rep. Prog. Phys. **79**, 094594 (2016).
22. S. Bhowal and I. Dasgupta, J. Phys.: Condens. Matter **33**, 453001 (2021).
23. V. J. Emery, Phys. Rev. Lett. **58**, 2794 (1987).
24. J. Hubbard, Proc. R. Soc. A **283**, 242 (1963).
25. Yu. A. Izyumov, Sov. Phys. Usp. **34**, 935 (1991).
26. Yu. A. Izyumov, Phys. Usp. **38**, 385 (1995).
27. Yu. A. Izyumov, Phys. Usp. **40**, 445 (1997).
28. N. N. Bogolyubov, Izv. Akad. Nauk SSSR, Ser. Fiz. **6**, 77 (1947).
29. D. N. Zubarev, *Non-Equilibrium Statistical Thermodynamics* (Nauka, Moscow, 1971; Mir, Moscow, 1973).
30. S. V. Tyablikov, *Methods in the Quantum Theory of Magnetism* (Nauka, Moscow, 1965; Plenum, New York, 1967).
31. J. Hubbard, Proc. R. Soc. A **285**, 542 (1965).
32. F. Dyson, Phys. Rev. **102**, 1217 (1956); Phys. Rev. **102**, 1230 (1956).
33. R. O. Zaitsev, Sov. Phys. JETP **41**, 100 (1975).
34. R. O. Zaitsev, Sov. Phys. JETP **43**, 574 (1976).
35. R. Zwanzig, Phys. Rev. **124**, 983 (1961).
36. H. Mori, Prog. Theor. Phys. **33**, 423 (1965).
37. M. M. Otrokov, I. I. Klimovskikh, H. Bentmann, et al., Nature (London, U.K.) **576**, 416 (2019); arXiv: 1809.07389 (2018).
38. D. Zhang, M. Shi, T. Zhu, et al., Phys. Rev. Lett. **122**, 206401 (2019).
39. Y. Gong, J. Guo, J. Li, et al., Chin. Phys. Lett. **36**, 076801 (2019).

Translated by N. Wadhwa